Effects of Streamwise Surface Treatments on Trailing Edge Noise Reduction

Abbas Afshari[1]
Yazd University, Yazd, Iran

Mahdi Azarpeyvand[2]
University of Bristol, Bristol, United Kingdom, BS8 1TR

Ali A. Dehghan[3]
Yazd University, Yazd, Iran

Máté Szőke[4]
University of Bristol, Bristol, United Kingdom, BS8 1TR

The use of surface treatments as a passive flow control method for trailing edge noise reduction is considered in this paper. In order to investigate the effects of different types of surface treatments on surface pressure fluctuations, eddy convection velocity and spanwise length scale, a long flat-plate model, equipped with several streamwise and spanwise surface pressure microphones has been designed and built. Measurements have been carried out for a variety of 2D and 3D surface treatments. The flow behavior downstream of the surface treatments is also studied by employing a single probe hotwire anemometer. Results indicated that the use of finlets with coarse spacing leads to a favorable reduction in PSD at mid to high frequencies and an undesirable increase in spanwise length scale. In the case of finlets with fine spacing, the high frequency pressure fluctuations have been effectively suppressed and the spanwise length-scale has been reduced, but with a penalty of low to mid frequency surface pressure elevation. Furthermore, it is found that the ratio of the finlets spacing to the boundary layer thickness is a critical parameter for achieving maximum surface pressure PSD reduction and the finlets spacing should be in the order of the boundary layer inner region. It has also been shown that the proposed novel 3D surface treatments have better aeroacoustic performance than the standard 2D ones in terms of the reduction in the surface pressure power spectral density, the longitudinal and lateral coherence and eddy convection velocity.

Nomenclature

c	=	flat plate chord, m
d	=	pinhole diameter, m, $d^+ = du_\tau/\nu$
f	=	frequency, Hz
f_c	=	crossing frequency, Hz
h	=	finlets height, m
p'	=	fluctuating surface pressure, Pa

[1] School of Mechanical Engineering, Yazd University, PhD student, *afshar.abbas@gmail.com*
[2] Department of Mechanical Engineering, University of Bristol, Senior Lecturer and Royal Academy of Engineering research fellow, *m.azarpeyvand@bristol.ac.uk*
[3] School of Mechanical Engineering, Yazd University, Associate Professor
[4] Department of Mechanical Engineering, University of Bristol, PhD student

S = spacing between finlets or riblets, m, $S^+ = Su_\tau/\nu$
t = trailing edge thickness, m
u = streamwise velocity, m/s, $u^+ = u/u_\tau$
U_c = convection velocity, m/s
u_{rms} = root mean square of velocity fluctuations, m/s
u_τ = wall-friction velocity, m/s
U_∞ = free stream velocity, m/s
x = streamwise distance from the flat plate leading edge, m
y = normal distance from the flat plate, m, $y^+ = yu_\tau/\nu$
z = lateral distance from the flat plate midspan, m
z_{min}, z_{max} = minimum and maximum lateral distance from the flat plate midspan, m
ϕ = surface pressure power spectral density, Pa^2/Hz
$\Lambda_{p,3}$ = spanwise length scale, m
δ = boundary-layer thickness, m
δ^* = boundary-layer displacement thickness, m
Δz = spanwise separation between microphones, m
ε = streamwise separation between microphones, m
γ_p^2 = coherence of Surface pressure fluctuations
ν = kinematic viscosity, m^2/s
τ = time delay, s
λ_h = convected hydrodynamic wavelength, m
PSD = Power Spectral Density
SPF = Surface Pressure Fluctuation
TE = Trailing Edge
ZPG = Zero Pressure Gradient

I. Introduction

Airfoil self-noise is produced when the airfiol interacts with the turbulent flow generated by the airfoil itself. Turbulent boundary layer trailing edge (TBL-TE) broadband noise is one of the most important airfoil self-noise mechanisms [1]. Over the recent decades, trailing edge noise has received considerable research attention in the form of theoretical, computational and experimental research works. The phenomena plays an important role in the noise generation in the field of aviation, wind turbines, turbo-machinery, etc [2-5].

Numerous theoretical trailing edge noise models have been developed over the past decades, a summary of which can be found in Ref. [2]. Formulations based on the linearized hydroacoustic methods are one of the basic approaches for the prediction of the far field trailing edge noise, and rely on the induced hydrodynamic pressure field at some distance upstream of the TE. The majority of trailing edge noise prediction methods have been formulated based on the surface pressure fluctuations as the unsteady surface pressure measurements can be easily made using flush-mounted unsteady pressure transducers. According to Amiet's [6] and Howe's [7] formulations, point spectra and the frequency dependent spanwise length scale of the surface pressure fluctuations (SPF), defining the efficiency of scattering at the TE, are crucial quantities in the prediction of the far-field trailing edge noise. Therefore, reducing the surface pressure spectrum level and the spanwise turbulent length scale in the TE region will result in the reduction of the trailing edge noise.

To reduce the turbulent boundary layer trailing edge noise, various passive airfoil noise control methods have been developed, such as trailing edge serrations [5, 8-21], trailing edge brushes [22-24], porous trailing edge [25-30], airfoil shape optimization [31, 32], trailing edge morphing [33, 34] and more recently upstream surface treatment [35-37]. It was shown both analytically [8-12] and experimentally [5, 13-21] that trailing edge noise levels can be reduced by modifying the trailing edge geometry with serrations so that the flow disturbances are scattered into sound with reduced efficiency. In fact, the addition of trailing edge serrations leads to a reduction in the effective spanwise length of the trailing edge. Flexible trailing-edge brushes have demonstrated a significant noise-reduction potential in wind-tunnel tests on flat plates and on a 2-D airfoil. Porous trailing edges can also significantly reduce the sound pressure level at low to mid frequencies. However, an increase in noise at higher frequencies was observed which was attributed to surface roughness effects. Moreover, brush and porous edge attachments may have practical limitations, namely the fine pores or spaces between brushes are prone to collect dirt and insects making them ineffective. Airfoil shape optimization such as modification of the thickness or the curve gradient can significantly affect the flow field around the airfoil, leading to improvement in both the aerodynamic

and aeroacoustic performance of the airfoil [31, 32]. Trailing-edge morphing can also effectively reduce the airfoil trailing edge noise over a wide range of flow speeds and angles of attack.

In 2014, Clark *et al*. [38] used a series of canopies, inspired by the owl's downy coating, over the rough surface to suppress roughness noise. All canopies were reported to have a strong influence on the surface pressure spectra, and attenuations of up to 30 dB were observed. This development represented a new passive method for roughness noise control. To investigate the applicability of this method in reducing trailing edge noise, Clark *et al*. [35], in 2015, examined over 20 variants of surface treatments by performing aeroacoustic wind tunnel measurements on a tripped DU96-W180 airfoil. The treatments were installed directly upstream of the trailing edge to modify the boundary layer turbulence prior to interacting by the edge. Compared to the untreated airfoil, the treatments were found to be effective, providing broadband attenuation of trailing edge noise of up to 10dB. Furthermore, the aerodynamic impact of the treatment appeared to be minimal. However, their investigation was limited to the far-field noise measurements. Later in 2016, Clark *et al*. [36], carried out a series of experiments which focused on more detailed measurements of the effects of finlets on the flow over the DU96 airfoil. Far-field noise spectra and beamforming maps were collected for a new set of finlet geometries in addition to those tested by Clark *et al.* [35]. Unsteady surface pressure data were collected near the trailing edge and between the finlets to better quantify their effects on the boundary layer turbulence. At the same time in 2016, Afshari *et al.* [37] studied the mechanisms responsible for the behaviors of the upstream surface treatments by simultaneous measurement of the surface pressure fluctuations and boundary layer velocity on a long flat-plate model, equipped with several streamwise and spanwise surface pressure microphones. They showed that using 2D finlets as surface treatments can lead to around 8 dB reduction of the surface pressure fluctuations near the trailing edge. More importantly, they observed that the spanwise coherence can be significantly reduced over a wide range of frequencies. Around 30% reduction of eddy convection velocity has also been reported. Furthermore, the correlation between the turbulent structures within the outer region of the boundary layer and the unsteady surface pressure exerted on the surface were reduced significantly by using treatments with height of only 10% of the boundary layer thickness. Although the models of the two studies (Clark *et al*. [35, 36] and Afshari *et al.* [37]) were different (one uses a DU96-W180 airfoil with adverse pressure gradient in trailing edge region and another a flat-plate with zero pressure gradient), they generally achieved the same results. However, obvious differences exist about the effects of changing the finlets spacing on the performance of the upstream surface treatments. Clark's results show that with decreasing the finlets spacing, their efficiency in reducing the far-field noise spectra at mid to high frequencies increases while Afshari's results show a reduction in the efficiency of the upstream surface treatments in reducing the surface pressure point spectra with reducing the finlets spacing.

The use of the surface treatment as a means of passive flow control has been a topic of intensive research during the last decades. The shape of these microstructure surface treatments, known as riblets, were imitated from one of the oldest species known as fast swimmers, sharks. Two dimensional streamwise riblets have been widely studied [39-42] and shown to be effective in reducing the turbulent skin friction drag by as much as 10%, given an optimal geometry of h/s ~0.5 for the blade riblets [41]. The drag reduction results are typically presented as a function of s^+ which represents the riblet spacing normalized with the wall shear velocity and the viscosity of the fluid. The results on the effect of lateral spacing s of riblets have shown that the highest drag reduction occurs at $s^+ \approx 15 - 17$ and therefore ribbed surfaces, which are used for drag reduction can be considered as transitionally rough [43]. Besides the 2D streamwise riblets, some studies have explored the effects of three-dimensional riblets such as the interlocking staggered riblets proposed by Bechert et al. [44] and showed that by inserting an additional fin into the groove, the drag reduction regime of the surface might be extended to higher s^+, but the actual drag reduced using 3D riblets was less than that of equivalent 2D riblets. In general, there are two mechanisms for the riblet drag reduction phenomenon. First, riblets impede the cross-stream translation of the streamwise vortices, which causes a reduction in vortex ejection and outer-layer turbulence. Second, riblets lift the vortices off the surface and reduce the amount of surface area exposed to the high-velocity flow [45]. However, it should be noted that despite the similarities between the drag reduction riblet and the noise reduction finlet, there are some differences between them too. Riblets dimensions are in order of viscous sublayer to affect the streamwise vortices, while the proposed surface treatments are larger in order to break-up the large coherent structures like the hairpin vortices or packages of large hairpins close to the trailing-edge.

Given the apparent similarities between the riblets (used to reduce drag) and the surface treatments (proposed for trailing edge noise reduction) and also due to the differences which exist between the effects of changing the finlets spacing on the performance of the upstream surface treatments, one can infer that there may be an optimum finlets spacing which can lead to the highest possible reduction in the surface pressure spectra level. Therefore, moving away from the optimum spacing leads to a reduction in the acoustic efficiency of the upstream surface treatments.

The work described in this paper is a continuation of Afshari *et al.* [37] work. In the present study, by employing a few extra surface treatments with various finlets spacing, the effects of the finlets spacing on the efficiency of the upstream surface treatments in reducing the surface pressure point spectra, the spanwise length scale and the convection velocity in the TE region are investigated. Moreover, to improve the efficiency of the standard 2D surface treatments, two different 3D novel surface treatment configurations has been introduced and tested. The experimental layout is described in section II and the main outcomes of the investigation are presented in section III.

II. Experimental setup

A. Wind tunnel and model

The experiments were carried out in the open subsonic wind tunnel of the Yazd University with a test section size of 46 × 46 × 240 cm. At the maximum speed of 25 m/s, the free stream turbulence intensity has been measured to be less than 0.3%. The wall-pressure fluctuations measurements are often carried out in an acoustically quiet wind tunnel to avoid noise contamination due to the wind tunnel background noise. In the present wind tunnel, the centrifugal forward blades type fan creates low broadband noise. By replacing the internal solid surfaces of the test section with an appropriate porous material (15 cm thickness) the background noise of the facility is reduced by up to 20 dB, making the working section suitable for this experiment.

The flat plate used in the present work has a chord length of 580 mm, a span of 456 mm and a thickness of 8 mm. The leading edge of the model is made to be elliptical with a semi-major axis of 12 mm and a semi-minor axis of 4 mm. Furthermore, to realize a ZPG turbulent boundary layer on the topside in the rear area, the trailing edge is asymmetrically beveled at an angle of 12 ° [46]. The model is composed of a main body and a detachable trailing edge part, which allows spanwise microphones to be installed horizontally inside the flat plate trailing edge section. The trailing edge plate is attached to the main body with two side plates. The thickness of the trailing edge is 0.4 mm and therefore the narrowband blunt trailing edge vortex shedding noise is negligible ($t/\delta^* < 0.3$) for all free-stream velocities considered in this study [3]. The experiments were carried out at zero angle of attack and for three different free stream velocities, $U_\infty = 10$, 15, and 20 m/s, corresponding to the momentum thickness based Reynolds numbers of $Re_\theta = 5900$, 8400, and 10500, respectively. The blockage ratio of the flat plate model is less than 2 % for all the experiments and hence the wind tunnel walls effects on the measured quantities is negligible [47]. To ensure fully developed turbulent boundary layer and to artificially thicken the boundary layer, the model was tripped by a step with 12 mm height block which was introduced at the 5 percent of the chord length downstream of leading edge on upper surface. The detailed CAD view of the flat plate model is shown in Fig. 1.

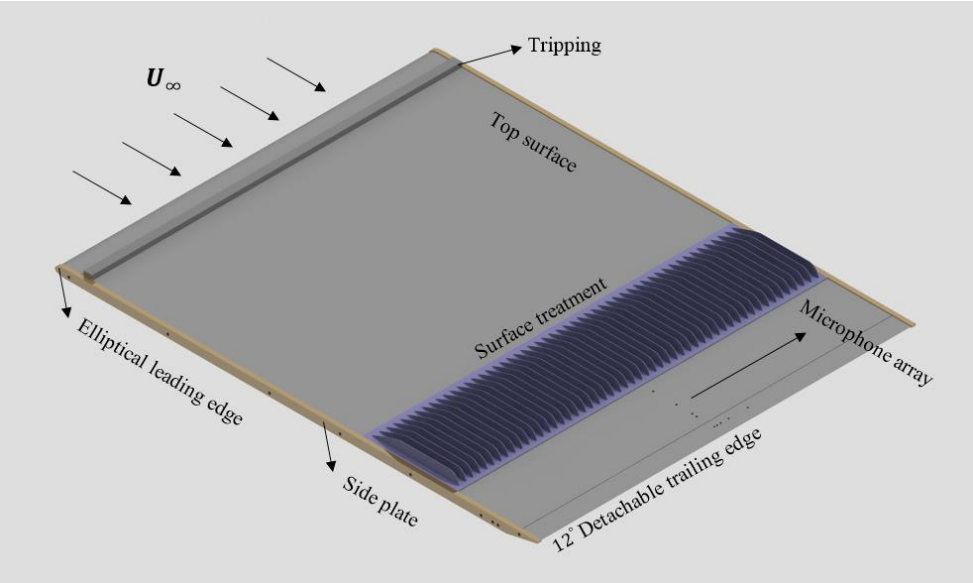

Fig. 1.The flat plate model with a detachable trailing edge, surface treatment, step trip and side plates.

B. Instrumentation

The FG-23329-P07 miniature microphones, manufactured by Knowles Acoustics, are employed for the measurement of the unsteady surface pressure. The microphones dimensions are 2.5mm in diameter, 2.5 mm height and with a circular sensing area of 0.8 mm. The same microphones had been used before in other experiments [48, 49] and have shown to be reliable for the frequencies considered in this study. The microphones are embedded in the flat plate under a pinhole mask of 0.4 mm diameter in order to decrease attenuation effects at high frequencies due to the finite size of the microphones sensing area. All pinholes are created with drilling the flat plate surface using an accurate drill machine. Two techniques have been used to embed microphones in the flat plate. For the positions far from the trailing edge, the plate is thick enough to embed microphones vertically under the pinhole. For the positions near the trailing edge, the microphones have been installed inside the flat plate parallel to the surface (i.e. horizontally). In this arrangement, each microphone was linked to its pin hole on the surface by a horizontal transmission tube. A schematic of both arrangements is depicted in Fig. 2.

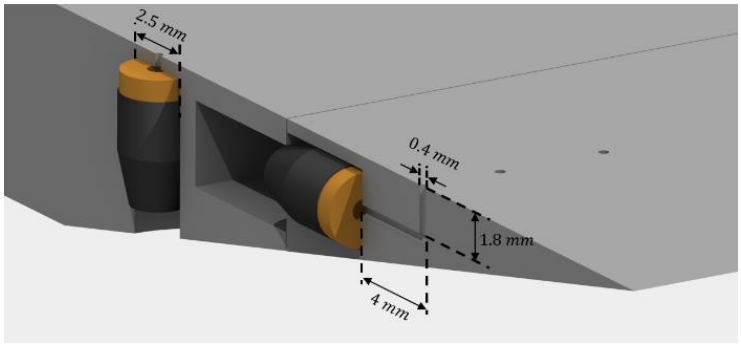

Fig. 2. Illustration of both microphones installation: under pin-hole configuration and with horizontal transmission tube configuration.

The issue of the resonant frequencies associated with the selected arrangements shown in Fig. 2 was studied analytically and experimentally to ensure that the resonant frequencies are outside the frequency range of interest. The frequency response (amplitude and phase) of both arrangements are presented in Fig. 3.

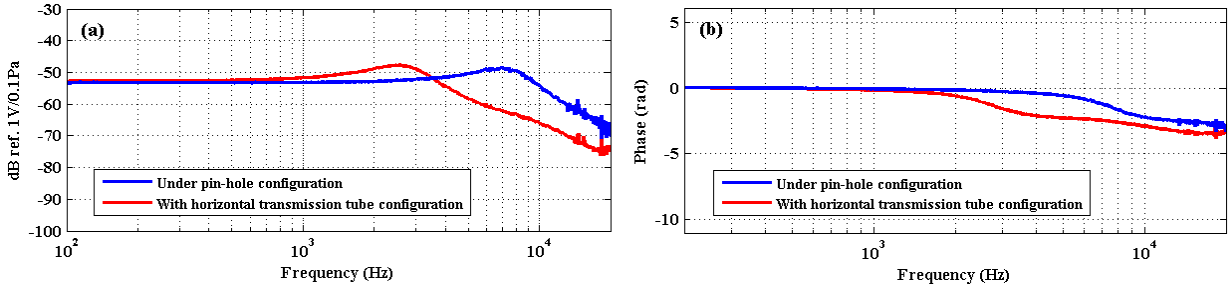

Fig. 3. Frequency response of the microphone in the pin-hole configuration (microphone No. 6) and microphone with horizontal transmission tube (microphone No. 4). (a) Amplitude (b) Phase.

C. Layout of surface microphone array

The Layout of the surface pressure microphone arrays is depicted in Fig. 4. The locations of the pinholes on the upper surface of the flat plate are summarized in Table 1. A total number of 9 microphones are arranged in the form of L-shaped array on the surface of flat plate. A set of microphones are distributed in the streamwise direction from x/c = 0.85 to 0.976 to provide information on the convection velocity of the turbulent eddies. Another set of microphones are distributed along the span to measure the spanwise length scale. The space between the surface microphones is not equal which leads to a non-redundant population of sensor spacing and maximizing the number of spatial lags available in a cross-correlation comparison.

Many investigations have been carried out to study the important parameters of the surface pressure microphone arrays, including the pinhole diameter, the distance of the spanwise microphones from the trailing edge and spanwise spacing of the pinholes [50-56]. The finite size of the pressure transducers leads to attenuation of the wall pressure fluctuations spectral levels at high frequencies as reported in references [50-52]. In fact, the pressure measured by transducers of finite size is the average pressure applied across the transducer sensing area and therefore pressure fluctuations smaller than the transducer sensing area are spatially integrated, and thereby attenuated. In order to resolve this issue usually a pinhole mask is used to decrease the effective sensing area of the pressure transducer. Typically, the transducer sensing diameter, scaled on inner-layer variables, $d^+ = du_\tau/\nu$, is used to determines whether the attenuation is significant. Schewe [53] concluded that $d^+ < 19$ is sufficient for the proper capturing of all essential wall pressure fluctuations. Later, Gravante *et al*. [54] reported that the maximum allowable non-dimensional sensing diameter to avoid spectral attenuation at high frequencies is in the range $12 < d^+ < 18$. The pinhole mask used for the current study for the free stream velocities ranging from 10 to 20 m/s, gives a non-dimensional sensing diameter range of $10 \leq d^+ \leq 19$. Thus, the error due to the attenuation effects can be assumed negligible. However, the correction suggested by Corcos [50] has been implemented to the data in order to account for any possible attenuation effects.

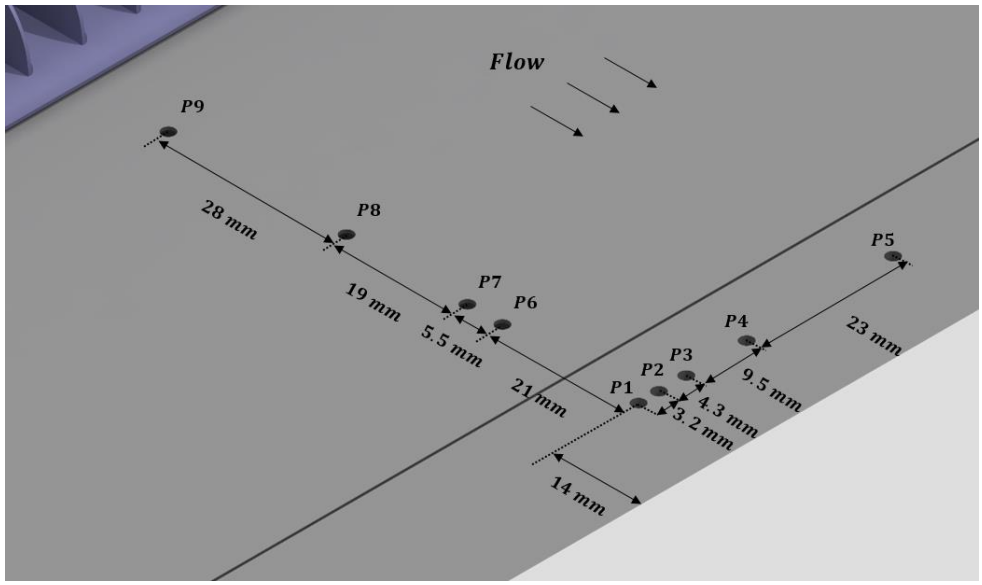

Fig. 4. Map of L-shaped surface microphone array.

Table 1. Position of pressure pinholes in the flat plate.

Microphone number	Distance from TE (mm)	Distance from midspan (mm)
p1, p2, p3, p4, p5	14.0	0.0, 3.2, 7.5, 17.0, 40.0
p6,p7,p8,p9	35.0, 40.5, 59.5, 87.5	0.0

Special care is taken in the selection of the distance of the spanwise microphones from the trailing edge. This distant must not be so small that the spanwise length scale $\Lambda_{p,3}(\omega)$ and $\phi(\omega)$, which represent statistical information about the incident pressure field, be affected by the scattering process at the trailing edge. On the other hand, it must be close enough to the trailing edge to be representative of the turbulence properties past the trailing edge. Ffowcs-Williams and Hall [55] and Brooks and Hodgson [56] reported that the minimum sensor distance to the TE where scattering effect can be neglected is about $\lambda_h/2$, where λ_h is the convected hydrodynamic wavelength of interest ($\lambda_h = U_c/f$). Therefore, due to this criterion and limitation of the minimum thickness at the flat plate TE for microphone installation, the spanwise pinholes are located at 14 mm upstream of the TE (at x/c = 0.976). Thus, it can be concluded that the measured surface pressure is not contaminated by the scattered pressure field above the 250, 375, and 500 Hz corresponding to the free stream velocities, $U_\infty = 10$, 15, and 20 m/s, respectively. The pinhole locations in the spanwise direction were arranged according to a potential function, *i.e.* $z/z_{min} = (z_{max}/z_{min})^{(i-2)/(N-2)}$, $i = 2..N$, in order to obtain a good range of distances with all pinhole pairs. z_{min} and z_{max} are the minimum and maximum lateral distances of the pinholes from the flat plate midspan and are 3.2 mm and 40 mm, respectively.

D. Surface treatments

In the present study, the blade-shaped fence (finlet) is chosen as the surface treatment for the flat plate. The design parameters of the finlets are illustrated in Fig. 5. The finlets are supported by thin substrates glued to the flat plate. The leading and trailing edges of the substrate was faired to the flat plate surface by covering it with 0.1mm thick aluminum tape. The surface treatment is placed on the top surface, upstream of the trailing edge, from x = 370 mm (x/c ≈ 0.64) to x = 475 mm (x/c ≈ 0.82). The profile of the finlet leading edge is designed to have the same geometry to that of the turbulent boundary layer shape so that the height of finlets, before reaching the maximum height, is proportional to $x^{4/5}$ (x starts from the finlet leading edge). To investigate the effects of finlets spacing, a total number of 5 standard 2D surface treatments with finlets spacing of 1 mm, 2 mm, 4 mm, 8 mm and 12 mm, with finlet height of 12 mm, were fabricated using rapid prototyping, Fig. 5a. Furthermore, to investigate the efficiency of the 3D surface treatments, two different surface treatments were fabricated, Figs. 5b and 5c. The staggered configuration consists of blade-shaped finlet elements arranged in an interlocking form (5b), while in the last configuration, the spacing between the finlets reduces gradually at several stages (5c).

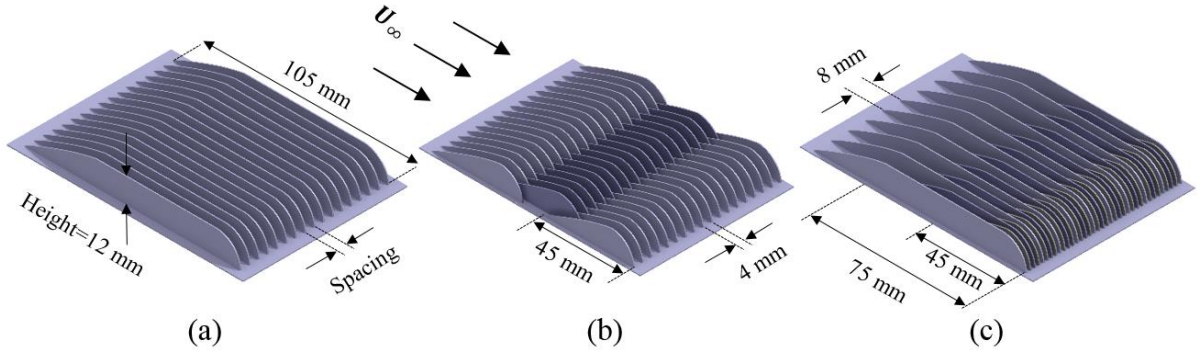

Fig. 5. Various surface treatment configurations. (a) 2D standard configuration, (b) 3D staggered configuration, (c) 3D gradual-change configuration.

E. Measurement procedure

The unsteady surface pressure measurements were performed with a total number of 9 FG-23329-P07 miniature microphones. A tube with a length of 110 mm and diameter of 10 mm along with a high quality loudspeaker were used for the calibration of the microphones. A ¼-inch G.R.A.S. Microphone Type 40BP, calibrated with a G.R.A.S. Sound Calibrator Type 42AB, was used as the reference microphone. The calibration results in the laboratory showed that the sensitivity of the FG-23329-P07 microphones varied approximately between 20 and 24.1 mV/Pa. To provide a transfer function for each microphone, all microphones have been calibrated in-situ with a white noise excitation signal over the frequency range of 200 Hz to 20 kHz. The attenuation and possible resonances induced by the horizontal transmission tubes used to connect the microphones to the pin-holes on the surface are therefore accounted for using this in situ calibration. The method employed in the calibration of the FG-23329-P07 microphones is based on the calibration procedure proposed by Mish [57]. The microphones were powered by a 10-channel power module (manufactured by the Electronics workshop at the Engineering Department of the Yazd University) and the data were collected by a 16-channel NI PCI-6023E data acquisition system. The sampling frequency was f_s = 40 kHz, and a total of 800,000 samples were recorded over 20 seconds. The spectral analysis of the recorded data is done using the pwelch power spectral density (PSD) function in MATLAB with a Hamming window function, 50% overlap and a reference pressure of 2×10^{-5} Pa. Reliable and repeatable measurements are achieved for all microphones.

In order to better understand the flow structure and the energy content of the turbulent structures, several velocity measurements have been performed in the boundary layer of the trailing edge using a single constant temperature hot-wire anemometer. The sensing element of probe is a standard 5μm diameter tungsten wire with a length of 1.25 mm. The probe was calibrated both statically and dynamically by a standard Pitot tube and a square-wave test procedure and all data were low-pass filtered at 30 kHz. The probe is traversed in the boundary layer or in the wake by using a three axis traverse unit controlled by stepper motors with 0.01 mm accuracy. The traverse unit allowed continuous movement in the streamwise (x), spanwise (z) and vertical (y) directions. The data were recorded at a sampling frequency of 40 kHz for a sampling time of 10 seconds. The spanwise flow velocity measurements confirmed an approximate 300-mm extent of uniform 2D flow conditions at x = 566 mm (x/c =

0.976). The mean velocities for locations y < 1 mm and skin friction coefficient are estimated using Spalding's equation [58],

$$y^+ = u^+ + e^{-\kappa B}\left[e^{\kappa u^+} - 1 - \kappa u^+ - (\kappa u^+)^2/2 - (\kappa u^+)^3/6\right] \quad (1)$$

where $u^+ = u/u_\tau$, $y^+ = yu_\tau/\nu$ and κ and B are the von-Karman and an additive empirical constant, which are chosen to be 0.41 and 5.0, respectively. Spalding's formula is a power-series interpolation scheme joining the linear sublayer to the logarithmic region. The friction velocity, u_τ is obtained by fitting the measured data to the logarithmic region of Spalding's equation [59].

III. Results and Discussion

Measurements were carried out at zero angle of attack for three different free-stream velocities, $U_\infty = 10$, 15, and 20 m/s, corresponding to the momentum thickness based Reynolds numbers of $Re_\theta = 5900$, 8400, and 10500, respectively. Since measurements at all flow speeds follow the same trend, only the results for U_∞=10 m/s is presented here. For all cases the flat plate boundary layers were fully turbulent, having been tripped as described in section II.A. The results of the 2D and 3D surface treatments are presented in the following sections.

A. Standard 2D surface treatment

Figure 6 shows the surface pressure power spectral density measured by TE microphone (p4) near the trailing edge of the baseline and treated flat plates (x/c=0.976) referenced to p_{ref} = *20 μPa* at U_∞=10 m/s (δ=75 mm). The microphone data are corrected based on the calibration procedure and Corcos correction [50] described in sections II.E and II.C. The results in Fig. 6 show the effects of the finlets spacing on surface pressure power spectral density compared to the baseline. The results for the coarse and fine spacings (S) are presented in Fig. 6a and Fig. 6b, respectively. As can be seen, the PSD behavior of the two categories are very different. For the finlets with coarse spacing (S=12 and 8 mm), the presence of upstream surface treatment leads to a reduction in the pressure PSD at mid to high frequencies with negligible changes in the low frequency domain. Furthermore, with decreasing the spacing between the finlets, their effectiveness in reducing the surface pressure power spectral density is increased, Fig. 6a. On the other hand, for the cases with fine spacing (S=4, 2 and 1 mm) results have shown that the presence of the upstream surface treatment leads to a reduction in the pressure PSD at high frequencies, Fig. 6b. However, at low to mid frequency domain an undesirable increase has been observed. As can be seen in Fig. 6b, with using fine spacing finlets, there is a cross frequency, f_c, below which the surface pressure PSD of the treated plate is higher than that of the smooth flat plate. Furthermore, by reducing the spacing between the finlets, the crossing frequency is seen to move to higher frequencies, resulting in an increase in the area where the spectra is elevated and hence the effectiveness of the upstream surface treatment in reducing the surface pressure power spectral density is decreased.

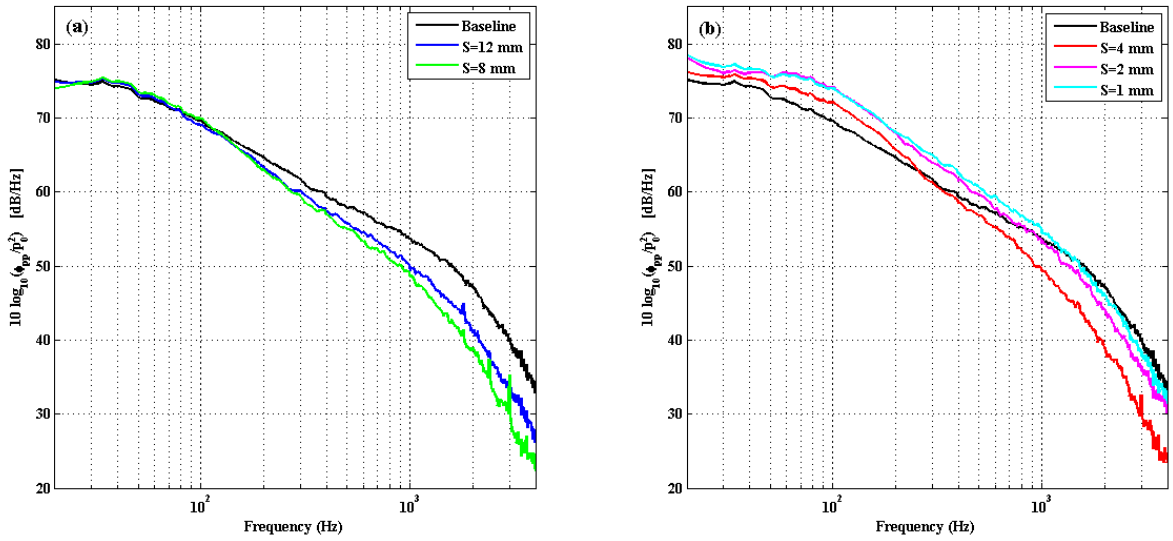

Figure 6. Surface pressure power spectral density referenced to p_{ref}=*20 μPa* measured by microphone p4 on the trailing edge of the tripped flat plate at U_∞=*10 m/s* (δ=*75 mm*). *Showing the effects of finlets spacing on surface pressure power spectral density compared to the Baseline.*

The turbulent flow field around the trailing edge is the source of the trailing edge noise. Therefore, to gain better insight into the mechanism through which both the coarse and fine spacing finlets affect the flow structure, velocity measurements near the trailing edge of the flat plate with and without surface treatments (baseline) are studied. Figure 7a shows the variation in the boundary layer mean velocity profile (u/U_∞) measured for the baseline and treated flat plate cases at the position of p4 microphone (x/c = 0.976) at U_∞=10 m/s (δ=75 mm). As shown in Fig. 7a, all surface treatments create a velocity deficit, indicating that they alter the downstream flow structures. Also, it can be observed that the variations in the boundary layer mean velocity profile increases with decreasing the space between the finlets, such that the finest surface treatment (with a spacing of 2 mm) creates the largest velocity deficit. The variation in the boundary layer turbulent intensity ($u_{\mathrm{rms}}/U_\infty$) measured for the baseline and treated flat plate is shown in Fig. 7b. As can be seen, for the cases with coarse spacing (S=8 mm), the turbulent intensity decreases as a result of the presence of the finlets. However, by decreasing the finlets spacing, an increase in the turbulence intensity at about $y/h \approx 1.25$ appears. It is hypothesized that this is due to the turbulence generated by the shear layer of the surface treatment wake. On the other hand, reducing the finlets spacing leads to more reduction of the turbulent intensity in the near wall regions. Once again, the finest finlets, with 2 mm spacing, provided the largest turbulence intensity reduction in the near wall region. Figure 7c shows the boundary layer mean velocity normalized with the inner layer scales for both the baseline and treated flat plate cases at the position of p4 microphone (x/c = 0.976). It has been observed that by reducing the finlets spacing, the variation in the boundary layer mean velocity profile increases such that the results for the finer finlets approaches that of backward steps [60, 61]. In other words, the flow behind the finlets with fine spacing behaves nearly like as the flow behind the backward steps. Results also show that the friction velocity decrease as a results of the upstream surface treatments. Furthermore, the reduction in the friction velocity increases with decreasing the space between the finlets.

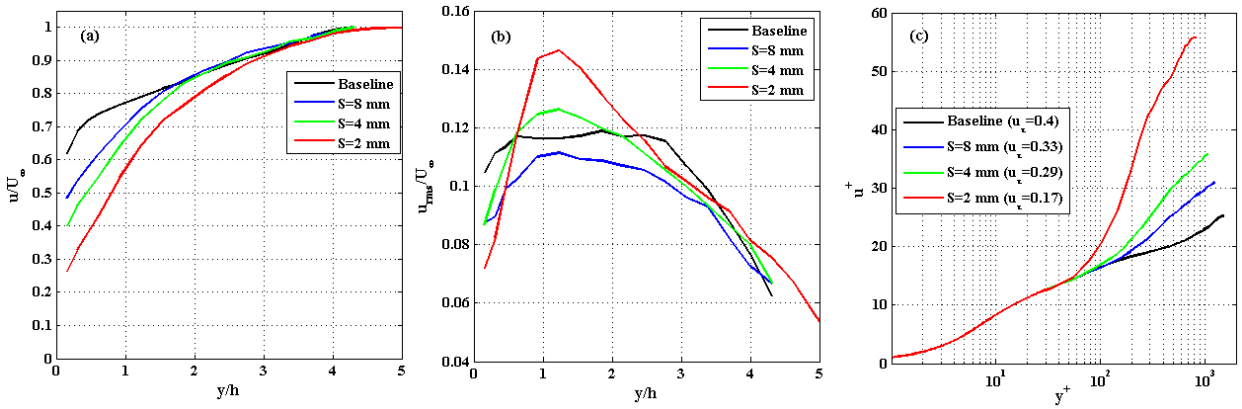

Figure 7. (a) Boundary layer mean velocity profiles normalized with free stream velocity and finlets height (b) turbulence intensity profiles normalized with finlets height (c) Boundary layer mean velocity normalized with inner layer scale at the position of microphone p4 (x/c = 0.976) at U_∞=10 m/s (δ=75 mm). *Showing the effects of finlets spacing on Boundary layer and turbulence intensity profiles compared to the Baseline.*

To investigate the differences between the boundary layer flow structure due to the presence of the surface treatments considered, the energy content of the turbulence structures has been studied. The velocity power spectral density (PSD) results have been measured at x/c=0.976 upstream of the trailing edge, *i.e.* at the position of the spanwise microphones at U_∞=10 m/s (δ=75 mm). Results are presented in Fig. 8 which demonstrate the PSD contour plots normalized with the results of the untreated flat plate (baseline) ($\Delta PSD_u = 10log_{10}(\Phi_{uu,treated}/\Phi_{uu,Baseline})$). It can be observed that for the case of coarse spacing (S=8 mm), in the near wall region ($y/h < 0.5$), the low frequency variation of the turbulence structures is negligible. However, at higher frequencies, the turbulence energy content of the flow, in this region, is significantly reduced. Furthermore, in the areas far away from the wall ($y/h > 0.5$), there are not notable changes in the turbulence energy. It is hypothesized that in the case of finlets with coarse spacing, the flow structures are able to pass through the finlets and therefore their energy is dissipated through friction and perhaps break-up of large structures. The contour of the velocity power spectral density reduction for the case of fine finlets spacing (S=2 mm), is demonstrated in Fig. 8b. As can be seen, in the areas near the wall ($y/h < 0.5$), the reduction in the turbulence energy content of the flow in the low frequency range is low and it increases at high frequency, even more than the case of coarse finlets spacing. This

increase compared to the coarse case is likely to be due to the increased surface area and therefore friction. However, in the region between $0.5< y/h < 2$, the turbulence energy content of the flow is significantly increased due to the additional turbulence generated in the shear layer initiated by separation regions formed at the finlets end [62]. Furthermore, there is a high energy region at low frequencies ($50< f < 100$) which is consistent with the surface pressure spectral results in Fig. 6b (S=2 mm). Therefore, for the case of fine finlets spacing, the flow separation and emergence of the high energy content region are believed to be responsible for the undesirable low frequency energy increase and also the reduction of the finlets effectiveness at high frequencies.

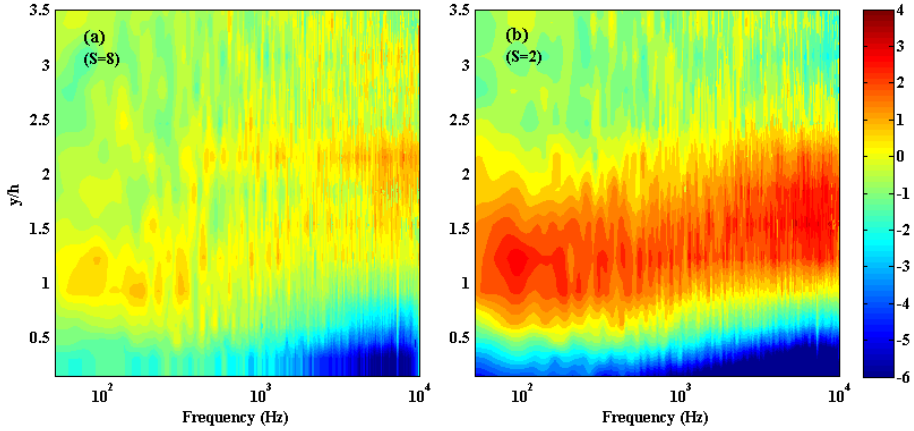

Figure 8. Normalized velocity power spectral density (PSD) contour plots of treated flat plate normalized with Baseline at 14 mm (x/c=0.976) upstream of the trailing edge at U_∞=10 m/s (δ=75 mm). *Showing the effects of finlets spacing on velocity power spectral density compared to the Baseline.* ($\Delta PSD_u = 10log_{10}(\phi_{uu,treated}/\phi_{uu,Baseline})$).

Based on the above discussion, the trend of the surface pressure power spectral density variations with changing the spacing between the finlets is not monotonic. For the finlets with coarse spacing, the coherent turbulent structures like the streamwise vortices, the hairpin vortices or even packages of large hairpins may be able to pass through the finlets and therefore their energy can be dissipated through friction. In these cases, reducing the spacing between the finlets leads to an increase in the surface area and therefore more reduction in the downstream surface pressure power spectral density is expected. Below a certain spacing value, the finlets begin to behave like a solid object and therefore the majority of the flow goes over the surface treatment instead of passing through the finlets. In these cases, the flow behind the surface treatment behaves nearly like the flow behind a backward step. In fact, part of the upstream boundary layer separates at the end corner of the finlets, forming a free-shear layer. Therefore, the spacing between the finlets should be sized such that while the surface area is maximized, the formation of the shear layer caused by the flow passing over the surface treatment is prevented. Thus, there is an optimum finlets spacing that leads to the highest PSD suppression in the high frequency region with minimum penalty of the PSD increase in the low to mid frequency region. As shown in Fig. 6, the optimum spacing (S) should be somewhere between 4 and 8 mm for the cases considered in this study.

To obtain a more general criterion for the optimum finlets spacing as a fraction of the boundary layer thickness, various experiments have been carried out for flows with various boundary layer thicknesses. To achieve various boundary layer thickness, the model was tripped by steps with different heights. In Fig. 9, the PSD results for treated flat plate, normalized with the results of the baseline case ($\Delta PSD_p = 10log_{10}(\phi_{pp,treated}/\phi_{pp,Baseline})$) are presented at a constant frequency of 2 kHz for several boundary layer thicknesses and finlet spacing. According to the results presented in Fig. 9a, with increasing the boundary layer thickness, the optimum finlet spacing increases and the amount of PSD reduction decreases. These variations are understandable since by increasing the boundary layer thickness, the dimension of the coherent turbulent structures increases and therefore larger finlet spacing will be required for allowing large flow structures to pass through the finlets. In Fig. 9b, the same data as in Fig. 9a are presented while the *x*-axis is normalized by the boundary layer thickness and the *y*-axis shows $PSD \times \delta/h$, where h is the height of the finlets. It can be seen that the data almost collapses onto a single curve showing that the optimum spacing finlets occurs at $S = 0.07\delta$. Therefore, to achieve maximum reduction in the surface pressure power spectral density, the spacing between the finlets should be in the order of the inner layer thickness.

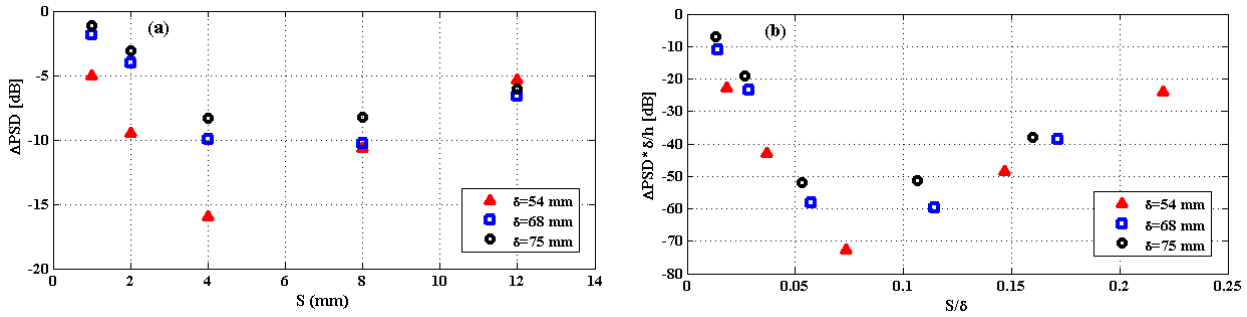

Figure 9. Surface pressure power spectral density (PSD) of treated flat plate normalized with Baseline measured by microphone p4 on the trailing edge of the tripped flat plate (with various trip) at U_∞=10 m/s. *Showing the effects of finlets spacing on surface pressure power spectral density reduction.* ($\Delta PSD_p = 10log_{10}(\phi_{pp,treated}/\phi_{pp,Baseline})$).

As reported by Brooks and Hodgson [56], the two types of longitudinal and lateral coherences are related to different aspects of the pressure field. The longitudinal coherence relates more specifically to the lifespan (or, inversely, the decay) of the eddies, whereas the lateral coherence relates to the physical size of the eddies. The two aspects are certainly interrelated since the structures with the largest scale have a longer lifespan. The effects of the finlets spacing on the longitudinal and lateral coherences, measured using the streamwise and spanwise microphones at U_∞=10 m/s (δ=75 mm) are presented in Figs. 10 and 11. As can be seen, the effects of the finlets spacing on the longitudinal and lateral coherences are completely different. For the coarse finlets spacing (S=12 and 8 mm), the presence of an upstream surface treatment leads to an increase in the longitudinal and especially lateral coherence at all frequencies. In fact, by passing the coherent turbulent structures through the finlets, their size and lifespan increases. However, when the spacing between the finlets is small (S=2 and 1 mm), the longitudinal and lateral coherences of the turbulent structures are significantly reduced, indicating that the large coherent turbulent structures have been successfully removed from the boundary layer. For S=4 mm, the longitudinal coherence is slightly reduced while the lateral coherence is not affected much.

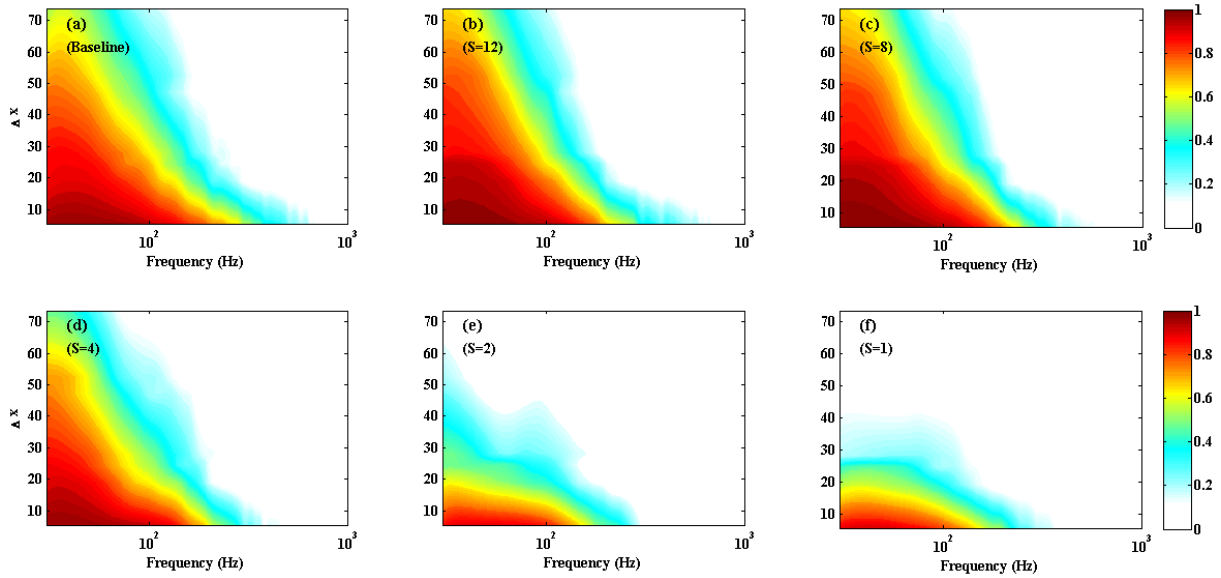

Figure 10. Contour plots of longitudinal coherence measured on the tripped flat plate between streamwise microphones at U_∞=10 m/s (δ=75 mm). *Showing the effects of finlets spacing on longitudinal coherence compared to the Baseline.*

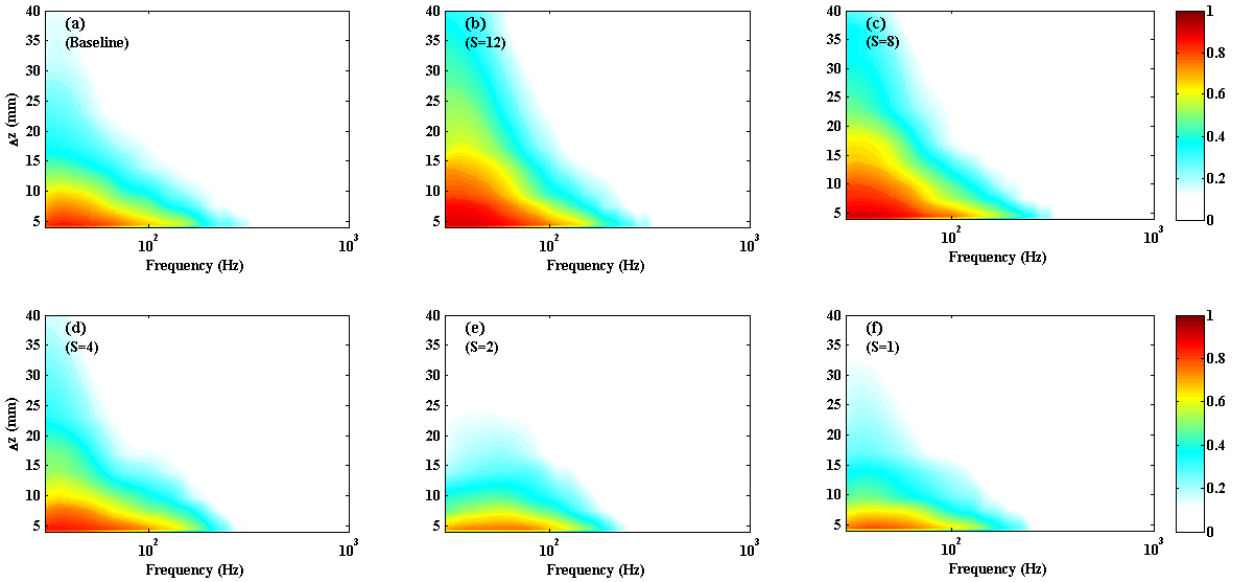

Figure 11. Contour plots of lateral coherence measured on the tripped Flat Plate between spanwise microphones at U_∞=10 m/s (δ=75 mm). *Showing the effects of finlets spacing on lateral coherence compared to the Baseline.*

In addition to the trailing edge surface pressure power spectral density, the frequency dependent spanwise length scale of the SPFs and the convection velocity in the TE region are also important quantities for determining of the far-field trailing edge noise. The spanwise length scale of the surface pressure fluctuations, $\Lambda_{p,3}(\omega)$, was calculated using the frequency dependent spanwise coherence $\gamma^2_{p,ij}(\omega,\Delta z)$, measured using the p1 to p5 microphones at x/c=0.976 at U_∞=10 m/s (δ=75 mm) ($\Lambda_{p,3}(\omega) = \int_0^\infty \gamma_{p,ij}(\omega,\Delta z)d\Delta z$). Figure 12 shows the effects of the finlets spacing on the calculated spanwise length scale. Results show that while the use of coarse finlets spacing (S=12 and 8 mm) leads to an increase in the spanwise length scale, the fine finlets spacing (S=2 and 1 mm) can reduce the spanwise length scale over a wide range of frequencies.

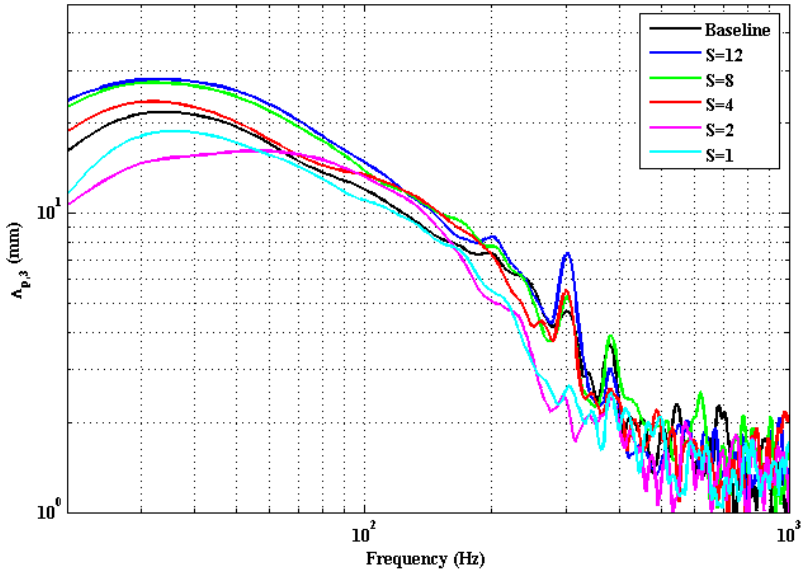

Figure 12. Spanwise length scales at U_∞=10 m/s (δ=75 mm). *Showing the effects of finlets spacing on spanwise length scale.*

Table 2 summarizes the values of the convection velocity of the turbulent eddies in the boundary layer, calculated using the phase analysis between the microphones p6 and p7 (ε=5.5 mm) near the trailing edge for the baseline and 2D treated cases at U_∞=10 m/s (δ=75 mm). It is clear from the results that the presence of the finlets leads to a reduction in the convection velocity. It is also seen that decreasing the finlets spacing causes more reduction of the convection velocity.

Table 2. Convection velocities calculated from the phase between microphone p6 and p7 (ε=5.5 mm) at U_∞=10 m/s (δ=75 mm).

Configuration	Baseline	(S=12)	(S=8)	(S=4)	(S=2)	(S=1)
U_C/U_∞	0.67	0.55	0.52	0.50	0.47	0.46

B. 3D novel surface treatment

The results of the standard 2D surface treatments revealed that by reducing the spanwise finlets spacing, the longitudinal and lateral coherences, the spanwise length scale and the eddy convection velocity can all be reduced. However, for the case of fine finlets spacing, further reducing the finlets spacing leads to a reduction in the efficiency of the surface treatment in reducing the surface pressure PSD, see Fig. 6b. As mentioned earlier, by reducing the finlets spacing, the finlets begin to behave like a solid backward step object and therefore the majority of the flow passes over the surface treatment, creating a strong shear layer behind the treatment. By combining finlets with different spacings and shapes in a 3D form, it might be possible to overcome this problem. Two types of 3D surface treatments have been used for this study. The geometry of the 3D treatments are described in section II.D. Figure 13 shows the surface pressure power spectral density obtained by employing various 2D and 3D surface treatments at U_∞=10 m/s (δ=75 mm). Results show that the proposed 3D surface treatments are more effective in reducing the pressure PSD at mid to high frequencies and they behave very similar to the 2D surface treatment with the finlets spacing of 4 mm. However, at lower frequencies, their behavior is somewhat different. Results have shown that the staggered configuration has a much better performance than the gradual-change type and minimizes the undesired low frequency noise increase.

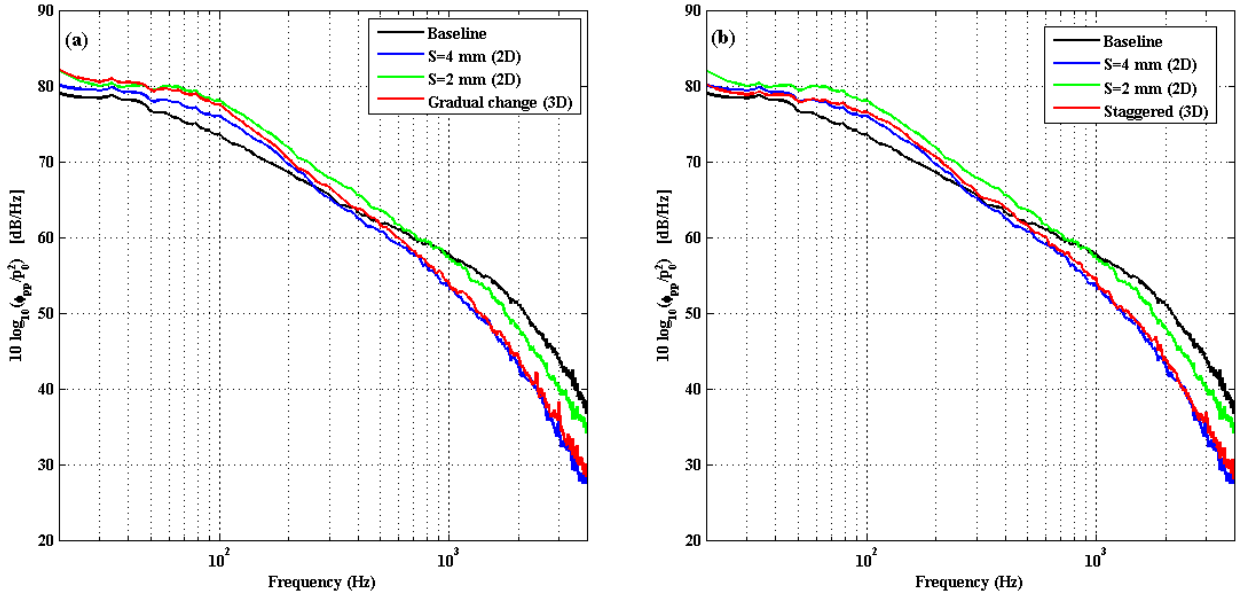

Figure 13. Surface pressure power spectral density referenced to p_{ref}=20 μPa measured by microphone p4 on the trailing edge of the tripped flat plate at U_∞=10 m/s (δ=75 mm). *Showing the effects of 3D novel surface treatments on surface pressure power spectral density.*

The longitudinal and lateral coherences measured using the streamwise and spanwise microphones for various 2D and 3D surface treatments at U_∞=10 m/s (δ=75 mm) are presented in Figs. 14 and 15, respectively. It is seen that

the effectiveness of both proposed 3D surface treatments especially the gradual-change type in reducing the longitudinal and lateral coherence is similar to the 2D surface treatment with the finlets spacing of 2 mm. Table 3 summarizes the values of the convection velocity of the turbulent eddies in the boundary layer calculated using the phase analysis between microphones p6 and p7 (ε=5.5 mm) near the trailing edge for the baseline and the proposed 3D novel surface treatments at U_∞=10 m/s (δ=75 mm). Results show that both 3D surface treatments are more effective in reducing the convection velocity than the 2D ones. Therefore, the novel proposed 3D surface treatments are more effective for noise reduction than the straight two-dimensional surface treatments.

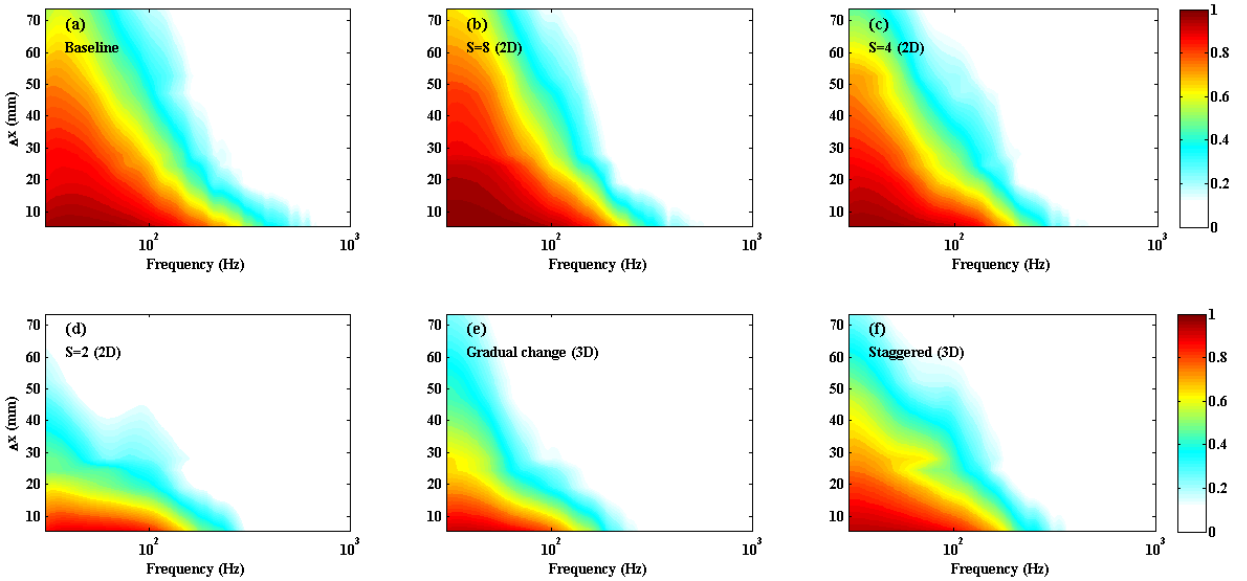

Figure 14. Contour plots of longitudinal coherence measured on the tripped Flat Plate between streamwise microphones at U_∞=10 m/s (δ=75 mm). *Showing the effects of 3D novel surface treatments on longitudinal coherence.*

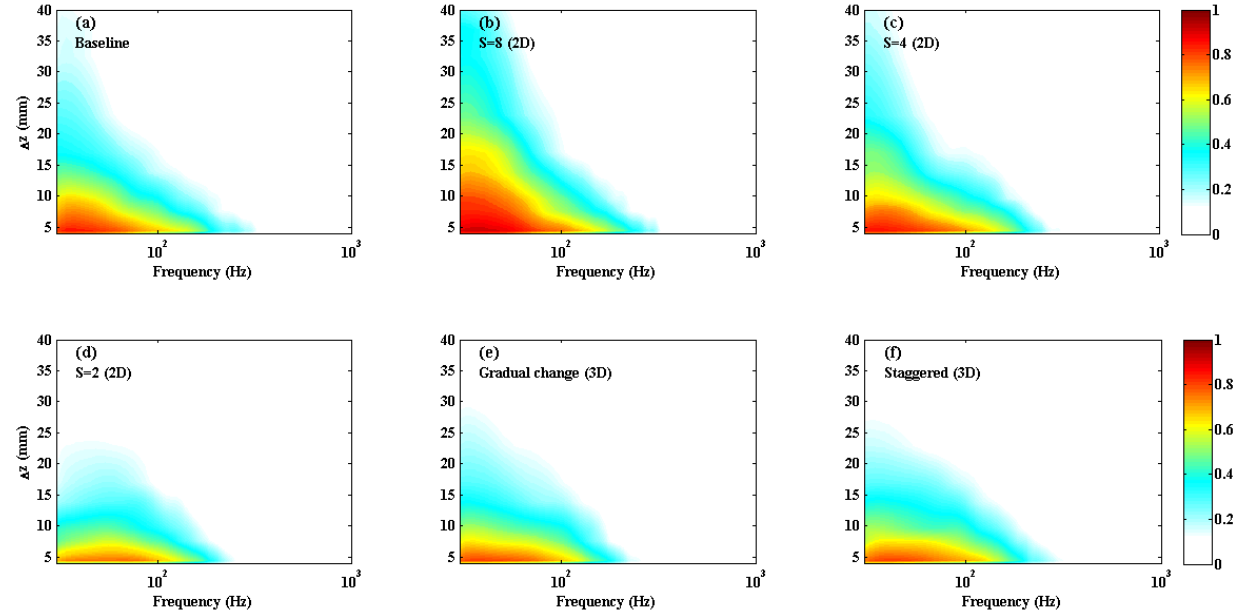

Figure 15. Contour plots of lateral coherence measured on the tripped Flat Plate between spanwise microphones at U_∞=10 m/s (δ=75 mm). *Showing the effects of 3D novel surface treatments on lateral coherence.*

Table 3. Convection velocities calculated from the phase between microphone p6 and p7 (ε=5.5 mm) at U_∞=10 m/s (δ=75 mm).

Configuration	Baseline	Gradual-change	Staggered
U_C/U_∞	0.67	0.42	0.45

IV. Conclusion

The present study is concerned with the experimental investigation of the surface treatments as a means of passive trailing edge noise control. The effects of finlets spacing on the surface pressure fluctuations, eddy convection velocity and spanwise length scale have been experimentally investigated using a long flat-plate model, equipped with several streamwise and spanwise surface pressure microphones. Results have revealed that the use of surface treatment with coarse spacing leads to a reduction in the surface pressure PSD at mid to high frequencies and an increase in the spanwise length scale. In the case of finlets with fine spacing, the high frequency pressure fluctuations have been effectively suppressed with a penalty of low to mid frequency elevation and proper reduction of spanwise length scale. Also, it is found that the ratio of the finlets spacing to the boundary layer thickness is a critical parameter for achieving maximum surface pressure power spectral density reduction. The mean velocity and turbulence intensity profiles measured downstream of the surface treatments showed that in all cases a significant velocity deficit occurs in the treated region, accompanied by a reduced turbulence intensity near the wall. However, by reducing the finlets spacing, an increase in the turbulence intensity at around $y/h \approx 1.25$ appears. It is believed to be due to the turbulence generated by the shear layer of the surface treatment wake. Furthermore, for the cases with fine spacing, the flow separation behind the treatment and emergence of the high energy content region at $0.5< y/h < 2$ are shown to be responsible for the undesirable low frequency energy increase and also reducing the finlet effectiveness. Results have also shown that while the coarser spacings increase the size and lifespan of the coherent turbulent structures, the use of the finer finlets leads to the break-up of large coherent structures. It has also been shown that the proposed novel 3D surface treatments can provide a better aeroacoustic performance than the standard 2D treatment in terms of reducing the surface pressure fluctuations, the longitudinal and lateral coherences and eddy convection velocity.

Acknowledgments

The second author (MA) would like to acknowledge the financial support of the Royal Academy of Engineering.

References

[1]Brooks, T. F., Pope, D. S., and Marcolini, M. A. *Airfoil self-noise and prediction*: National Aeronautics and Space Administration, Office of Management, Scientific and Technical Information Division, 1989.

[2]Roger, M., and Moreau, S. "Trailing edge noise measurements and prediction for subsonic loaded fan blades," *AIAA paper* Vol. 2460, 2002.

[3]Blake, W. "Mechanics of flow-induced sound and vibration. Volume 1 General concepts and elementary source. Volume 2-Complex flow-structure interactions," *Aplikace Matematiky, Applied Mathematics* Vol. 17, 1986.

[4]Lockhard, D. P., and Lilley, G. M. "The airframe noise reduction challenge," *Tech. Rep. NASA/TM-2004-213013, NASA Langley Research Center*, 2004.

[5]Oerlemans, S., Fisher, M., Maeder, T., and Kögler, K. "Reduction of wind turbine noise using optimized airfoils and trailing-edge serrations," *AIAA journal* Vol. 47, No. 6, 2009, pp. 1470-1481.

[6]Amiet, R. "Noise due to turbulent flow past a trailing edge," *Journal of sound and vibration* Vol. 47, No. 3, 1976, pp. 387-393.

[7]Howe, M. "A review of the theory of trailing edge noise," *Journal of Sound and Vibration* Vol. 61, No. 3, 1978, pp. 437-465.

[8]Howe, M. "Noise produced by a sawtooth trailing edge," *The Journal of the Acoustical Society of America* Vol. 90, No. 1, 1991, pp. 482-487.

[9]Azarpeyvand, M., Gruber, M., and Joseph, P. "An analytical investigation of trailing edge noise reduction using novel serrations," *19th AIAA/CEAS aeroacoustics conference*. Berlin, Germany, 2013, p. 2009.

[10]Sinayoko, S., Azarpeyvand, M., and Lyu, B. "Trailing edge noise prediction for rotating serrated blades," *20th AIAA/CEAS Aeroacoustics Conference*. Atlanta, GA, 2014, p. 3296.

[11]Lyu, B., Azarpeyvand, M., and Sinayoko, S. "A trailing-edge noise model for serrated edges," *21st AIAA/CEAS Aeroacoustics Conference*. Dallas, TX, 2015, p. 2362.

[12]Lyu, B., Azarpeyvand, M., and Sinayoko, S. "Prediction of noise from serrated trailing edges," *Journal of Fluid Mechanics* Vol. 793, 2016, pp. 556-588.

[13]Dassen, T., Parchen, R., Bruggeman, J., and Hagg, F. "Results of a wind tunnel study on the reduction of airfoil self-noise by the application of serrated blade trailing edges," *Proc. of the European Union Wind Energy Conference and Exhibition* Göteborg, Sweden, 1996.

[14]Braun, K., Van der Borg, N., Dassen, A., Gordner, A., and Parchen, R. "Noise reduction by using serrated trailing edges," *European wind energy conference*. Dublin, Ireland, 1997, pp. 472-475.

[15]Braun, K., Van der Borg, N., Dassen, A., Doorenspleet, F., Gordner, A., Ocker, J., and Parchen, R. "Serrated trailing edge noise (STENO)," *European wind energy conference*. Nice, France, 1999, pp. 180-183.

[16]Gruber, M., Azarpeyvand, M., and Joseph, P. F. "Airfoil trailing edge noise reduction by the introduction of sawtooth and slitted trailing edge geometries," *20th International Congress on Acoustics*. Sydney, Australia, 2010, p. 686.

[17]Gruber, M., Joseph, P., and Azarpeyvand, M. "An experimental investigation of novel trailing edge geometries on airfoil trailing edge noise reduction," *19th AIAA/CEAS Aeroacoustics Conference*. Berlin, German, 2013, p. 2011.

[18]Moreau, D., Brooks, L., and Doolan, C. "On the noise reduction mechanism of a flat plate serrated trailing edge at low-to-moderate Reynolds number," *18th AIAA/CEAS aeroacoustics conference* Colorado Springs, CO, 2012, p. 2186.

[19]Moreau, D. J., and Doolan, C. J. "Noise-reduction mechanism of a flat-plate serrated trailing edge," *AIAA journal* Vol. 51, No. 10, 2013, pp. 2513-2522.

[20]Liu, X., Azarpeyvand, M., and Theunissen, R. "Aerodynamic and aeroacoustic performance of serrated airfoils," *21st AIAA/CEAS Aeroacoustics Conference*. Dallas, TX, 2015, p. 2201.

[21]Liu, X., Kamliya Jawahar, H., Azarpeyvand, M., and Theunissen, R. "Wake development of airfoils with serrated trailing edges," *22nd AIAA/CEAS Aeroacoustics Conference*. Lyon, France, 2016, p. 2817.

[22]Herr, M., and Dobrzynski, W. "Experimental Investigations in Low-Noise Trailing Edge Design," *AIAA journal* Vol. 43, No. 6, 2005, pp. 1167-1175.

[23]Herr, M. "Experimental study on noise reduction through trailing edge brushes," *New Results in Numerical and Experimental Fluid Mechanics V*. Springer, 2006, pp. 365-372.

[24]Finez, A., Jondeau, E., Roger, M., and Jacob, M. C. "Broadband noise reduction with trailing edge brushes," *16th AIAA/CEAS Aeroacoustics Conference*. Stockholm, Sweden, 2010, p. 3980.

[25]Bohn, A. "Edge noise attenuation by porous-edge extensions," *14th Aerospace Sciences Meeting*. Washington, DC, U.S.A., 1976, p. 80.

[26]Howe, M. "On the added mass of a perforated shell, with application to the generation of aerodynamic sound by a perforated trailing edge," *Proceedings of the Royal Society of London A: Mathematical, Physical and Engineering Sciences*. Vol. 365, 1979, pp. 209-233.

[27]Fink, M., and Bailey, D. "Model tests of airframe noise reduction concepts," *6th Aeroacoustics Conference*. Hartford, CT, U.S.A., 1980, p. 979.

[28]Geyer, T., Sarradj, E., and Fritzsche, C. "Measurement of the noise generation at the trailing edge of porous airfoils," *Experiments in Fluids* Vol. 48, No. 2, 2009, pp. 291-308.

[29]Geyer, T., and Sarradj, E. "Trailing edge noise of partially porous airfoils," *20th AIAA/CEAS Aeroacoustic Conference*. Atlanta, GA, 2014, p. 3039.

[30]Showkat Ali, S. A., Szoke, M., Azarpeyvand, M., and Ilário, C. "Trailing Edge Bluntness Flow and Noise Control Using Porous Treatments," *22nd AIAA/CEAS Aeroacoustics Conference*. Lyon, France, 2016, p. 2832.

[31]Jones, B. R., Crossley, W. A., and Lyrintzis, A. S. "Aerodynamic and aeroacoustic optimization of rotorcraft airfoils via a parallel genetic algorithm," *Journal of Aircraft* Vol. 37, No. 6, 2000, pp. 1088-1096.

[32]Göçmen, T., and Özerdem, B. "Airfoil optimization for noise emission problem and aerodynamic performance criterion on small scale wind turbines," *Energy* Vol. 46, No. 1, 2012, pp. 62-71.

[33]Ai, Q., Azarpeyvand, M., Lachenal, X., and Weaver, P. M. "Aerodynamic and aeroacoustic performance of airfoils with morphing structures," *Wind Energy*, 2016, pp. 1325-1339.

[34]Ai, Q., Kamliya Jawahar, H., and Azarpeyvand, M. "Experimental investigation of aerodynamic performance of airfoils fitted with morphing trailing edges," *54th AIAA Aerospace Sciences Meeting*. San Diego, California, USA, 2016, p. 1563.

[35]Clark, I. A., Alexander, W. N., Devenport, W. J., Glegg, S., Jaworski, J. W., Daly, C., and Nigel, P. "Bio-Inspired Trailing Edge Noise Control," *21th AIAA/CEAS Aeroacoustics Conference*. Dallas, TX, 2015, p. 2365.

[36]Clark, I., Baker, D., Alexander, W. N., Devenport, W. J., Glegg, S. A., Jaworski, J., and Peake, N. "Experimental and theoretical analysis of bio-inspired trailing edge noise control devices," *22nd AIAA/CEAS Aeroacoustics Conference*. Lyon, France, 2016, p. 3020.

[37]Afshari, A., Azarpeyvand, M., Dehghan, A. A., and Szőke, M. "Trailing Edge Noise Reduction Using Novel Surface Treatments," *22nd AIAA/CEAS Aeroacoustics Conference*. Lyon, France, 2016, p. 2834.

[38]Clark, I., Devenport, W. J., Jaworski, J., Daly, C., Peake, N., and Glegg, S. A. "The noise generating and suppressing characteristics of bio-inspired rough surfaces," *20th AIAA/CEAS Aeroacoustics Conference*. Atlanta, GA, 2014, p. 2911.

[39]Walsh, M., and Weinstein, L. "Drag and heat transfer on surfaces with small longitudinal fins," *11th Fluid and PlasmaDynamics Conference*. Seattle, WA, U.S.A., 1978, p. 1161.

[40]Walsh, M. "Turbulent boundary layer drag reduction using riblets," *20th aerospace sciences meeting*. Orlando, FL, U.S.A., 1982, p. 169.

[41]Bechert, D., Bruse, M., Hage, W., Van der Hoeven, J. T., and Hoppe, G. "Experiments on drag-reducing surfaces and their optimization with an adjustable geometry," *Journal of fluid mechanics* Vol. 338, 1997, pp. 59-87.

[42]Lee, S.-J., and Lee, S.-H. "Flow field analysis of a turbulent boundary layer over a riblet surface," *Experiments in fluids* Vol. 30, No. 2, 2001, pp. 153-166.

[43]Jiménez, J. "Turbulent flows over rough walls," *Annu. Rev. Fluid Mech.* Vol. 36, 2004, pp. 173-196.

[44]Bechert, D., Bruse, M., and Hage, W. "Experiments with three-dimensional riblets as an idealized model of shark skin," *Experiments in fluids* Vol. 28, No. 5, 2000, pp. 403-412.

[45]Dean, B., and Bhushan, B. "Shark-skin surfaces for fluid-drag reduction in turbulent flow: a review," *Philosophical Transactions of the Royal Society of London A: Mathematical, Physical and Engineering Sciences* Vol. 368, No. 1929, 2010, pp. 4775-4806.

[46]Mosallem, M. "Numerical and experimental investigation of beveled trailing edge flow fields," *Journal of Hydrodynamics, Ser. B* Vol. 20, No. 3, 2008, pp. 273-279.

[47]Barlow, J. B., Rae, W., and Pope, A. "Low-speed wind tunnel testing, John Wiely & Sons." 3 ed., Wiley, New York, 1999.

[48]Garcia-Sagrado, A., and Hynes, T. "Wall-Pressure Sources Near an Airfoil Trailing Edge Under Separated Laminar Boundary Layers," *AIAA Journal* Vol. 49, No. 9, 2011, pp. 1841-1856.

[49]Gruber, M. "Airfoil noise reduction by edge treatments." PhD thesis, University of Southampton, 2012.

[50]Corcos, G. "Resolution of pressure in turbulence," *The Journal of the Acoustical Society of America* Vol. 35, No. 2, 1963, pp. 192-199.

[51]Willmarth, W., and Roos, F. "Resolution and structure of the wall pressure field beneath a turbulent boundary layer," *Journal of Fluid Mechanics* Vol. 22, No. 01, 1965, pp. 81-94.

[52]White, P. H. "Effect of Transducer Size, Shape, and Surface Sensitivity on the Measurement of Boundary-Layer Pressures," *The Journal of the Acoustical Society of America* Vol. 41, No. 5, 1967, pp. 1358-1363.

[53]Schewe, G. "On the structure and resolution of wall-pressure fluctuations associated with turbulent boundary-layer flow," *Journal of Fluid Mechanics* Vol. 134, 1983, pp. 311-328.

[54]Gravante, S., Naguib, A., Wark, C., and Nagib, H. "Characterization of the pressure fluctuations under a fully developed turbulent boundary layer," *AIAA journal* Vol. 36, No. 10, 1998, pp. 1808-1816.

[55]Williams, J. F., and Hall, L. "Aerodynamic sound generation by turbulent flow in the vicinity of a scattering half plane," *Journal of Fluid Mechanics* Vol. 40, No. 04, 1970, pp. 657-670.

[56]Brooks, T. F., and Hodgson, T. "Trailing edge noise prediction from measured surface pressures," *Journal of sound and vibration* Vol. 78, No. 1, 1981, pp. 69-117.

[57]Mish, P. F. "Mean loading and turbulence scale effects on the surface pressure fluctuations occurring on a NACA 0015 airfoil immersed in grid generated turbulence." M.S. Thesis, Virginia Polytechnic Institute and State University, 2001.

[58]Spalding, D. "A single formula for the "law of the wall"," *Journal of Applied Mechanics* Vol. 28, No. 3, 1961, pp. 455-458.

[59]Kendall, A., and Koochesfahani, M. "A method for estimating wall friction in turbulent boundary layers," *25th AIAA Aerodynamic Measurement Technology and Ground Testing Conference*. San Francisco, California, 2006, p. 3834.

[60]Bradshaw, P., and Wong, F. "The reattachment and relaxation of a turbulent shear layer," *Journal of Fluid Mechanics* Vol. 52, No. 01, 1972, pp. 113-135.

[61]Casarella, M. "Effects of surface irregularity on turbulent boundary layer wall pressure fluctuations," *ASME Journal of Vibration, Acoustics, Stress, and Reliability in Design* Vol. 106, No. 3, 1984, pp. 343-350.

[62]Ji, M., and Wang, M. "Aeroacoustics of turbulent boundary-layer flow over small steps," *48th AIAA aerospace sciences meeting including the new horizons forum and aerospace exposition*. Orlando, Florida, 2010, p. 6.